# Coherent Control of the Polarization of an Optical Field

S. Wielandy* and Alexander L. Gaeta
*School of Applied and Engineering Physics, Cornell University, Ithaca, New York 14853*
(Received 16 March 1998)

Through use of quantum coherence in an atomic system, we demonstrate that an optical field can be used to completely control the polarization state of another field. Theoretical and experimental results show that by applying a field with a frequency tuned near one transition, an initially isotropic atomic vapor can be made to behave as a linearly or circularly birefringent material for fields tuned near an adjoining transition. [S0031-9007(98)07434-1]

PACS numbers: 42.50.Gy, 32.80.Qk, 42.25.Ja

Phenomena resulting from quantum coherence have been the subject of great recent interest. The essential feature of these phenomena is that an atomic coherence is induced in a multilevel quantum system by applying a strong "control" laser field which alters the response of the system to a "probe" laser field. The resulting change in the imaginary part of the susceptibility experienced by the probe laser can result in electromagnetically induced transparency (EIT) [1], and has lead to the demonstration of an inversionless laser [2]. The corresponding change in the real part of the susceptibility allows for the control of self-focusing effects [3,4] and for large changes of the refractive index with no corresponding increase in absorption [5–7].

In this Letter, we use quantum coherence to provide complete and efficient control over the polarization state of a probe field. We show that an initially isotropic atomic vapor can be made to exhibit either linear or circular birefringence near one atomic transition by tuning a control field near another optical transition. Polarization rotation in a three-level atomic system was observed by Liao and Bjorklund [8], but the rotation in these experiments is a result of resonant enhancement of the dispersion associated with a two-photon transition rather than of a quantum coherence. Moreover, the intensities necessary to produce a significant rotation by this method ($\sim 10^6$ W/cm$^2$) required the use of pulsed lasers. Circular birefringence resulting from atomic coherences has been observed to produce small polarization rotations [9,10], but these experiments suffered from significant absorption loss and produced rotations of at most a few degress. Using our technique, we are able to change the polarization state of a probe beam from linear to any desired polarization state with very high efficiency by coherently inducing either linear or circular birefringence. This work represents a qualitative improvement over previous research with important implications because it allows light-induced polarization control at intensities accessible by continuous-wave lasers and because the high efficiency makes feasible the contruction of practical optical devices. A possible application of coherent polarization control is its use in conjunction with a polarizing beam splitter as a two-port optical switch. Moreover, in a suitable atomic system this technique allows for the construction of wave plates that operate in the deep UV and other wavelength regimes where none are currently available [11].

We consider the three-level ladder scheme shown in Fig. 1(a). The coherence-induced polarization control we observe is a direct result of the selection rules governing transitions between the magnetic sublevels that are coupled by the control and probe fields. Figure 1(b) shows the energy level scheme including magnetic sublevels (neglecting fine-structure and hyperfine-structure interactions) and demonstrates how the presence of a linearly polarized control field can result in birefringence for the probe beam. If the $z$ axis of the system is taken to be along the polarization direction of the control field, then this field will couple only the $m_l = 0$ sublevel of the $P$ state to the upper state. A probe field that is also $z$ polarized couples the ground state to this sublevel as shown by the solid arrow in Fig. 1(b) and can experience EIT and a coherently induced change in the refractive index. A probe field that is polarized in a direction orthogonal

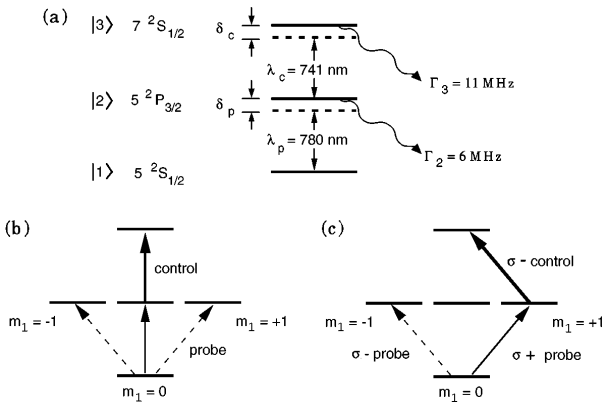


FIG. 1. (a) Energy level scheme for the ladder system. Also shown are the corresponding states and wavelength separations for atomic rubidium. (b) shows the magnetic sublevels coupled by a $z$-polarized control field; the solid arrow on the lower transition shows the sublevels coupled by a $z$-polarized probe field, and the dashed arrow shows the sublevels coupled by an orthogonally polarized probe field. (c) shows the sublevels coupled by a $\sigma-$ control field; the solid arrow shows the sublevels coupled by a $\sigma+$ probe field, and the dashed arrow shows the sublevels coupled by a $\sigma-$ probe field.

  

to the $z$ axis couples the ground state to the $m_l = \pm 1$ sublevels as shown by the dashed arrow in Fig. 1(b) and therefore experiences a refractive index unaffected by the presence of the control field. The net result is that the control field causes the ladder system to behave as a birefringent material with an optic axis determined by the polarization axis of the control field. A similar analysis illustrates how the control field can be used to produce circular birefringence as shown in Fig. 1(c). If the control laser is $\sigma-$ polarized, it couples only the $m_l = 1$ sublevel of the $P$ state to the upper state with the result that $\sigma+$ probe light experiences a coherently induced change in the refractive index while $\sigma-$ probe light experiences no change. In this case the net result is that the control field causes the system to behave as an optically active material with a chirality that is determined by the sense of polarization of the control field.

Our three-level ladder system is experimentally realized by a vapor cell of Rb atoms with the energy levels shown in Fig. 1. The probe is tuned near the $5\ ^2S_{1/2} \rightarrow 5\ ^2P_{3/2}$ D2 transition at a wavelength of 780 nm, and the control field is tuned near the $5\ ^2P_{3/2} \rightarrow 7\ ^2S_{1/2}$ transition at a wavelength of 741 nm. A schematic of the apparatus is shown in Fig. 2. The Rb vapor cell is 5 mm thick and is operated at a fixed temperature $T$ between 50 and 100 °C. The control transition is driven by a single-frequency (linewidth of 5 MHz) Ti:sapphire laser beam which produces up to 1 W of power at the Rb cell focused to a waist of 80 $\mu$m. The probe transition is driven by a linearly polarized 1-$\mu$W beam from a single-frequency (linewidth of 4 MHz) external-cavity diode laser focused to a spot size of 40 $\mu$m. Two-photon-Doppler cancellation is achieved with counterpropagating pump and probe beams. The transmitted probe beam is separated from the control beam via a dichroic mirror at an angle of incidence less than 1.5° to assure that the polarization state of the probe is not disturbed upon reflection from the mirror. The polarization of the control laser beam can be varied via a rotating polarizer and a quarter wave plate, and data are taken by scanning the frequency of the diode laser and recording the detected probe transmission on a digital oscilloscope. Frequency calibration of the laser scan is obtained by using the known hyperfine splitting and isotope shifts of the Rb $5\ ^2S_{1/2}$ ground state. All data presented here are associated with transitions from the $F = 2$ hyperfine level of the $^{85}$Rb $5\ ^2S_{1/2}$ ground state.

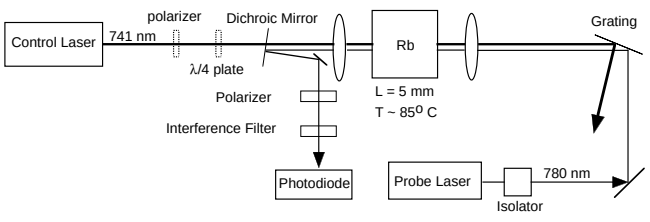


FIG. 2. Schematic of the experimental setup.

The experimental results shown in Fig. 3 demonstrate the flexibility of our technique in controlling the polarization of the probe. We plot as a function of the probe detuning from resonance the transmission of the probe field, after exiting the cell, through various polarization analyzers for the case in which the probe beam is initially linearly polarized. The transmission is defined such that unity transmission corresponds to the detected probe power with no analyzer when the probe is tuned far from resonance. Optimal efficiency in polarization control is found to occur for a nonzero control field detuning from resonance $\delta_c$, and in Figs. 3(a)–3(c), the control field is tuned to produce the maximum transmission through the polarization analyzer. In agreement with our theoretical analysis discussed below, we observe that the birefringence experienced by the probe field does not depend on the intensity of the control field in a simple manner since both the magnitude and location of the peak birefringence vary with the strength of the control field. For the data shown here, a fixed control field power of 300 mW is used. Figure 3(a) shows the probe transmission through a polarizer whose transmission axis is orthogonal to the initial polarization of the probe laser for a control field linearly polarized at 45° to the probe's initial polarization direction. For a probe detuning near 1.1 GHz, the system behaves as a $\lambda/2$ wave plate oriented at 45° to the initial probe polarization as demonstrated by the large transmission through the crossed polarizer. At a lower atomic density, we observe that the system can operate as a $\lambda/4$ wave plate, as shown in Fig. 3(b) in which we plot

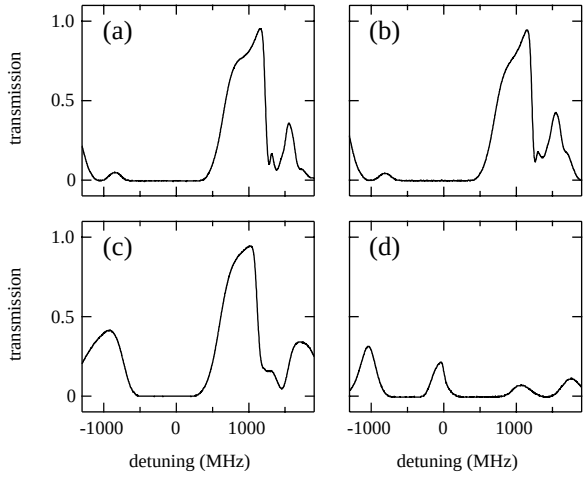


FIG. 3. Experimentally measured probe transmission as a function of probe detuning from resonance. In (a)–(c) the control field detuning is $\delta_c = 1.3$ GHz. (a) shows the transmission through an orthogonal analyzing polarizer when a control field linearly polarized at a 45° angle to the polarization axis of the probe is applied; (b) shows the transmission through a circular polarization analyzer when the same control field is applied at a lower atomic density; (c) shows the transmission through a crossed analyzing polarizer when a circularly polarized control field is applied; (d) repeats the experiment of (a) but with $\delta_c = 0$. In (a), (c), and (d) the temperature is 90 °C, and in (b) it is 80 °C.

the probe transmission through a circular-polarization analyzer. In Fig. 3(c), we use a circularly polarized control field to induce circular birefringence and again show the probe transmission through a crossed polarizer. Greater than 94% transmission through the polarization analyzer is achieved in all of the above cases at a probe detuning of approximately 1.1 GHz and over a bandwidth of more than 500 MHz. Together the results show that we are able to use the control field to place the probe field in any specified polarization state with high efficiency. It is interesting to note that the phase shift necessary to produce the polarization changes we observe implies a minimum change of $\sim 10^{-4}$ in the index of refraction for one polarization component of the probe beam with at most 6% absorption. This result is comparable to the largest reported value [6] of a coherently induced index change and in our case requires no incoherent pumping mechanism.

As described above, all of the polarization-control effects we observe here rely on the fact that one polarization component of the probe field (in either the linear or the circular basis) experiences a susceptibility that is directly modified by the presence of the control field, while the other component experiences a susceptibility that is unchanged. One can understand why it is desirable to operate with a nonresonant control field by considering the real and imaginary parts of the susceptibility for an ordinary, Doppler-broadened atomic resonance shown by the dashed curves in Figs. 4(a) and 4(b). These curves correspond to the susceptibility for the "control-blind" component of the probe field. The other polarization component of the probe is coupled to a magnetic sublevel of the intermediate state which is ac-Stark split into two dressed states that are a superposition of levels $|2\rangle$ and $|3\rangle$. The energies of these dressed states are shifted with respect to the energy of the unperturbed intermediate state in a manner that depends on the strength of the control field, characterized by the Rabi frequency $\Omega_c = 2\mu E_c/\hbar$, and on the control field detuning $\delta_c$. These energy shifts manifest themselves as a change in the susceptibility for one polarization component of the probe field, and can lead to satellite absorptive and dispersive features in the susceptibility spectrum as shown by the solid curves in Figs. 4(a) and 4(b). The satellite features allow the susceptibility for one component of the probe field to be manipulated by the application of an appropriate control field. Choosing the operating regime for optimal birefringence requires that two conditions be simultaneously met. First, it is necessary that the induced refractive index difference $\Delta n$ for the two polarization components of the probe beam be sufficiently large that the difference in the optical path length ($\Delta nL$, where $L$ is the interaction length) for the two components should be on the order of $\lambda$ for some probe field detuning range. Second, the system should be nearly lossless over this same detuning range so that the absorption for both components of the probe is small. We define a figure of merit for this system that is equal to the ratio of the refractive index difference between the two polarization components of the probe field and the corresponding residual absorption. Once this ratio is optimized, an arbitrary optical path length difference can be achieved by adjusting the atomic density. To minimize the absorption of the control-blind component of the probe field, it is desirable to operate at a relatively large probe detuning. To simultaneously achieve large birefringence, it is necessary to operate with a large control field detuning, which places the induced satellite dispersive feature at an appropriate location in the probe detuning spectrum. Since the control-induced satellite absorption peak falls off more rapidly than the corresponding refractive index change, substantial birefringence

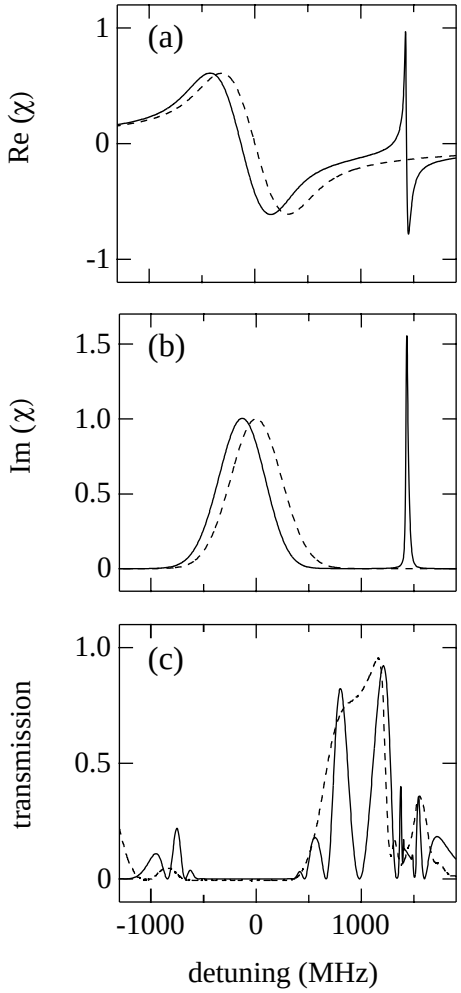


FIG. 4. Theoretically calculated probe susceptibility and transmission for a $z$-polarized control field. (a) shows the real part of the susceptibility experienced by the probe beam, and (b) shows the imaginary part. In (a) and (b), the solid line represents the susceptibility experienced by the $z$-polarized component of the probe, and the dashed line represents that experienced by the orthogonally polarized component. The solid line in (c) shows the predicted probe transmission through an orthogonal analyzing polarizer with the initial polarization of the probe taken to be linear and at an angle of 45° with respect to polarization axis of the control field. The dashed line in (c) shows the corresponding experimental data from Fig. 3(a) for comparison.

with negligible absorption can be achieved. To illustrate the value of operating with a nonresonant control field, Fig. 3(d) shows the experimentally observed transmission through a polarizer with its transmission axis orthogonal to the probe laser's initial polarization axis, reproducing exactly the conditions of Fig. 3(a) except with the control field tuned to resonance. The maximum probe transmission with the control field on resonance is less than 32%, compared to more than 94% with a detuned control field. The nearly lossless birefringence we achieve is possible only with a detuned control field and represents a qualitative improvement in both method and efficiency over earlier experiments on coherently induced birefringence [9,10]. In previous work on two-photon-induced circular birefringence [8], the observed birefringence can be interpreted as a result of the $\chi^{(3)}$ response of the atomic system [12]. In our scheme, we operate completely beyond the $\chi^{(3)}$ limit such that the resulting birefringence has a complicated dependence on the intensity of the control field. Changing the control field intensity changes both the size and location of the satellite features in the probe susceptibility described above and therefore changes not only the magnitude of the induced birefringence, but also the probe detuning at which optimal birefringence occurs.

To demonstrate that the simple model we outline above qualitatively describes the behavior we observe experimentally, we model the case of our coherently induced half-wave plate. The real and imaginary parts of the susceptibility for the probe both with and without the control field are calculated from the relevant density-matrix equations in the weak-probe limit [13] with the parameters given in Fig. 1(a) for Rb, and a Doppler average is performed over a Maxwell-Boltzman velocity distribution. These results are shown in Figs. 4(a) and 4(b). The complete polarization state of the probe after interaction with the ladder system is determined from the calculated susceptibilities, which allows for the prediction [Fig. 4(c)] of the transmission through a crossed polarizer. An experimental measurement of $\alpha_0 L$ with the control field off provides a calibration constant for the calculated susceptibility and allows quantitative predictions to be made by the theory. The experimental conditions from our experiment that are used in our simulation are $T = 90\,^{\circ}\mathrm{C}$, $\alpha_0 L = 28$, $\delta_c = 1300$ MHz, and $\Omega_c = 870$ MHz. The value used for $\Omega_c$ is inferred from the control field-induced ac-Stark splitting of the intermediate state measured at a smaller value of $\alpha_0 L$. Comparison of Figs. 3(a) and 4(c) shows that reasonable qualitative agreement exists between experiment and theory. In particular, this simple model predicts the detuning at which maximum birefringence occurs and the bandwidth over which significant birefringence is observed. The theoretical data show several oscillations in the transmission of the probe not found in the experimental data. These oscillations are a result of the large and varying birefringence experienced by the probe in this spectral region which induces a large phase difference between the two polarization components of the probe (i.e., $> \pi$). Thus, the probe transmission undergoes several oscillations as the probe's frequency is scanned, resulting from the fact that its polarization axis oscillates between an orientation that is parallel to the transmission axis of the polarization analyzer and one that is orthogonal to it. Our model does not consider the significant complications in the energy level scheme introduced by the fine and hyperfine structure that are present in our experiment, which we believe is the primary reason for the lack of quantitative agreement between our experiment and the predictions of the model. The addition of fine- and hyperfine structure affects the system in several ways. For a fixed control-field intensity, there is a range of corresponding Rabi frequencies that describe the varying coupling strengths between the various hyperfine levels and magnetic sublevels that compose levels $|2\rangle$ and $|3\rangle$ in our model. Moreover, the hyperfine splittings of levels $|2\rangle$ and $|3\rangle$ result in a range of control-field detunings of more than 300 MHz for transitions between the various hyperfine levels. Our simulations indicate that the combined result of these two effects is primarily to increase the bandwidth over which there is large birefringence, which is consistent with our experimental observations. The selection rules within the more complex level structure also complicate the analysis since in general no polarization component of the probe field will be completely control-blind. Nonetheless, even when considering the full hyperfine structure of our atomic system there persists an asymmetry in the effective coupling strength of the control field for various sublevels of level $|2\rangle$ that results in a coherently induced birefringence for the probe field.

In conclusion, we demonstrate the first use of quantum coherence to provide complete and efficient control over the polarization state of a probe field. We find that the process is optimized by operating with the control field detuned from resonance and present a model based on a simplified energy-level structure that provides a good qualitative understanding of our results.

This work was supported by the U.S. Office of Naval Research.

*Department of Physics, Cornell University, Ithaca, New York 14853.

[1] K.-J. Boller, A. Imamoglu, and S. E. Harris, Phys. Rev. Lett. **66**, 2593 (1991).
[2] A. S. Zibrov *et al.*, Phys. Rev. Lett. **75**, 1499 (1995).
[3] R. R. Moseley *et al.*, Phys. Rev. Lett. **74**, 670 (1995).
[4] M. Jain *et al.*, Phys. Rev. Lett. **75**, 4385 (1995).
[5] M. O. Scully, Phys. Rev. Lett. **67**, 1855 (1991).
[6] A. S. Zibrov *et al.*, Phys. Rev. Lett. **76**, 3935 (1996).
[7] S. E. Harris, Opt. Lett. **19**, 2018 (1994).
[8] P. F. Liao and G. C. Bjorklund, Phys. Rev. Lett. **36**, 584 (1976).
[9] Y. I. Heller *et al.*, Phys. Lett. **82A**, 4 (1981).
[10] F. S. Pavone *et al.*, Opt. Lett. **22**, 736 (1997).
[11] S. E. Harris (private communication).
[12] A. E. Kaplan, Opt. Lett. **8**, 560 (1983).
[13] J. Gea-Banacloche *et al.*, Phys. Rev. A **51**, 576 (1995).